Electrical Characteristics of Benzenedithiol versus Methylbenzenthiol Self-Assembled Monolayers in Multilayer Graphene-Electrode Molecular Junctions

Yeonsik Jang[1], Hyunhak Jeong[1], Dongku Kim[1], Wang-Taek Hwang[1], Inho Jeong[2], Hyunwook Song[2], Heejun Jeong[3, *], Misook Min[1, *], and Takhee Lee[1, *]

[1]*Department of Physics and Astronomy, Seoul National University, Seoul 08826, Korea*
[2]*Department of Applied Physics, Kyung Hee University, Yongin-si, Gyeonggi-do 17104, Korea*
[3]*Department of Applied Physics, Hanyang University, Ansan, Gyeonggi-do 15588, Korea*

We report our recent results of fabrication and characterization of molecular electronic devices using benzene-based self-assembled monolayers (SAMs) and multilayer graphene (MLG) electrodes as the top electrode. In particular, we compared the electrical characteristics of two different benzenethiol molecules; 4-methylbenzenethiol (MBT) and benzene-1,4-dithiol (BDT), which have the same backbone structure but different end-group. From the analysis, we found that the electrical characteristics of the devices showed no significant difference. We investigated that the background of this result is a physiorbed contact properties between graphene electrode and molecular layer.

Keywords: Molecular Devices, Multilayer Graphene (MLG), Benzenethiols.

1. INTRODUCTION

Molecular electronics utilizing molecular junctions as an active device component have been extensively studied with various fabrication techniques.[1–6] Specifically, vertical-type solid state device-structure metal-molecule-metal junctions have gained a significant attention as a general test-bed for studying charge transport characteristics and for the practical application of molecular electronic devices.[7–10] However, such fabrication technique usually incorporates evaporating top metal directly onto the molecular layer, which may easily cause filamentary path formation resulting in electrical short circuit in the junctions.[11–13] To deal with this problem, various methods for fabricating reliable molecular junctions have been reported using protective interlayer such as conducting polymer (PEDOT:PSS; poly(3,4-ethylenedioxythiophene) polystyrene sulfonate),[14] multilayer graphene (MLG),[15] and reduced graphene oxide (rGO),[16, 17] or using non-evaporating techniques such as direct metal transfer (DMT) method.[18, 19]

In this study, we fabricated benzenethiol-based solid-state molecular electronic devices using MLG electrodes as top interlayer-electrode between top Au metals and molecular monolayers. Specifically, we investigated two different benzenethiol molecules; 4-methylbenzenthiol (MBT) and benzene-1,4-dithiol (BDT), which have the same backbone structure but different end-group (MBT has –CH$_3$ and BDT has –SH). From the statistical analysis of fabricated devices, we found that there was no significant difference of electrical behavior of these two different types of molecular devices. This effect resulted from the physiorbed contact properties between graphene and molecule's end-group.

2. EXPERIMENTAL DETAILS

Figure 1(a) presents a schematic of device structure which was previously reported by our group.[15] On a p-type (100) Si substrate covered with 300 nm SiO$_2$, Au (30 nm)/Ti (5 nm) bottom electrodes were patterned using shadow mask by electron beam evaporator at a deposition rate of ~0.2 Å/s. Two different types of benzenethiols, MBT and BDT purchased from sigma-aldrich were self-assembled on 2 μm radius circular hole made
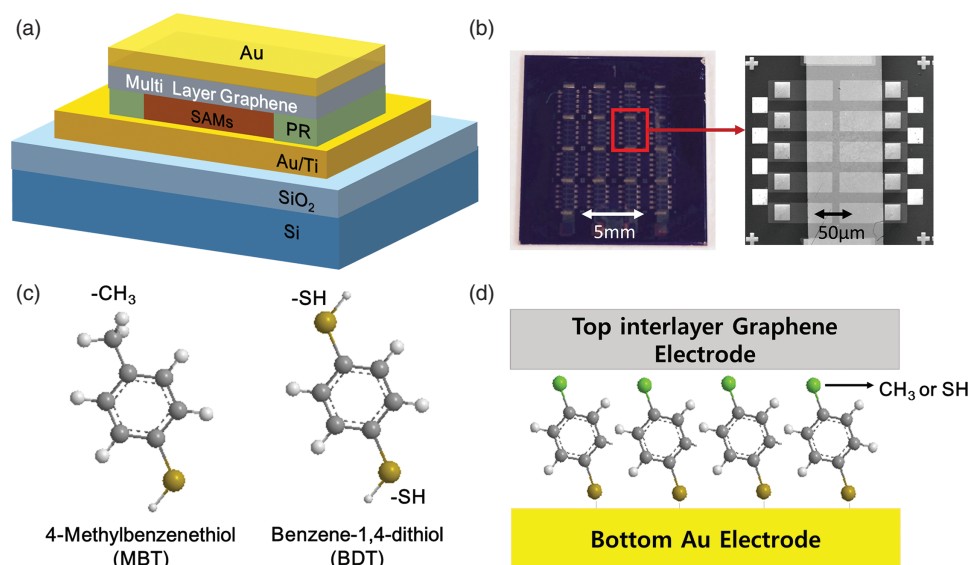
Figure 1. (a) Schematic of device structure. (b) Optical and SEM images of fabricated devices. (c) Molecular structures of MBT and BDT. (d) Structure of molecular junction.

by photolithography through photoresist wall (photoresist material of AZ5214E purchased from Az Electronic Matirials). We used 5 mM MBT and BDT solutions diluted with ethanol, then immersed samples in these solutions for 3 hours in a nitrogen-filled glove box. After molecular deposition, the samples were thoroughly rinsed with ethanol and dried in the glove box. MLG films were grown on 1.5×1.5 cm^2 Si substrate covered with Ni (300 nm)/Ti (10 nm) layer by chemical vapor deposition technique with gas flows of 200 sccm hydrogen and argon, and 15 sccm methane for 10 min at 900 °C under 20 Torr pressure. Then, poly(methyl methacrylate) (PMMA) was spin-coated onto the graphene film. After PMMA coating, we attached a support tape (thermal release sheet, purchased from Graphene-square) on the PMMA/MLG film. The Ni layer on the substrate was etched in an aqueous FeCl$_3$ solution. Then, the MLG film was transferred onto the SAM layer of the device. After transfer, unnecessary PMMA and supporting tape were removed by acetone. After that, top Au electrode (15 nm) were patterned using shadow mask by electron beam evaporator at a rate of ~0.1 Å/s.

Finally, oxygen plasma treatment (10 sccm, 50 W) was performed to remove remaining MLG film for prohibiting direct pathway through top and bottom electrodes. The electrical measurements were performed with a semiconductor parameter analyzer (Keitheley 4200 SCS) and a probe station system (JANIS Model ST-500). Figure 1(b) shows optical and scanning electron microscope (SEM) images of fabricated molecular devices. Figure 1(c) shows the chemical structures of MBT and BDT. They have the same backbone structure but different end group (–CH$_3$ for MBT and –SH for BDT). Figure 1(d) shows structures of our molecular junctions.

3. RESULTS AND DISCUSSION

We performed statistical analysis to distinguish electrical properties between the two types of molecules. To do so, we fabricated enough number of molecular devices (120 devices for each molecular type) for analysis. Figure 2(a) shows a histogram of Log$_{10}$ (current density (J)) values at 1 V measured from all BDT and MBT molecular devices except electrical short or open and fabrication failure. The working devices were determined by using a Gaussian function fitting. We defined 'working' devices as those included in the interval of 3σ ranges between $\mu + 3\sigma$ and $\mu - 3\sigma$, where μ is mean and σ is standard deviation of Gaussian fitting curve. We found that logarithmic mean current densities of MBT and BDT molecular devices at 1 V are not significantly different (3.86 for MBT and 4.00 for BDT) but BDT has
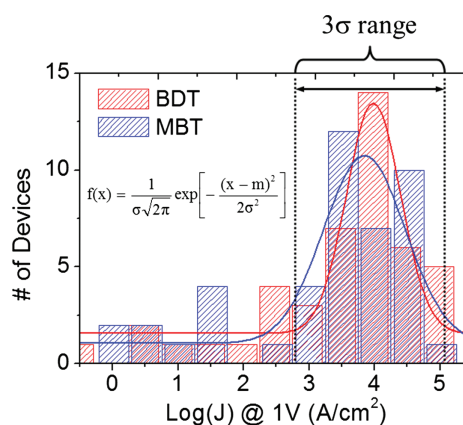

Figure 2. A histogram of Log$_{10}$ (current density (J)) values at 1 V measured from all BDT and MBT molecular devices.

Table I. Summary of the statistical analysis for the fabricated devices.

Molecules	# of devices	Fab. failure	Short	Open	Non Working	Working	Device yield
BDT	120	28	32	12	13	35	69
(%)	(100)	(23.3)	(26.7)	(10.8)	(8.1)	(29.1)	(28.8)
MBT	120	15	43	18	10	34	
(%)	(100)	(12.5)	(38.5)	(15)	(8.3)	(28.3)	

a slightly higher current density within a range of error bars. In Table I, the statistical analysis results for MBT and BDT molecular devices are summarized. In this study, the device yield was determined to be 69/240 ($\sim$30%), which is lower than that of our group's previous report for alkanethiol-based molecular junctions with MLG electrode ($\sim$90%).[15] However, the device yield in this study showed much higher than that of pure metal-molecule-metal junctions ($\sim$1%),[13, 20] so that it can be regarded that MLG film plays a proper role as a protective interlayer. Naturally, the higher device yield is anticipated to be obtained through more delicate graphene transfer technique. Note that conjugated π-bonding benzenethiol molecular orbitals lie near on the Fermi level of electrode, therefore they form relatively lower tunneling barrier than σ-bonding alkane molecules.

Figure 3(a) shows statistical current density–voltage (J–V) data of working BDT and MBT molecular devices

with MLG electrodes. The error bars are the standard deviation. The BDT molecular junctions showed a slightly higher conductance than MBT junctions. However, the error ranges between the two types of molecular junctions were overlapped each other, which means the difference of conductance between them is not significantly distinguishable. The inset graph in Figure 3(a) shows one representative J–V data for MBT junction measured right after fabrication and 30 days after being stored in ambient condition. This graph presents the stability of molecular devices with MLG electrode. Figure 3(b) is Arrhenius plot (J vs. inverse temperature) for BDT and MBT molecular devices at various temperatures from 120 to 300 K and voltages from 0.6 to 1 V. The temperature independence of the molecular devices suggests that the main transport mechanism is tunneling through a molecular tunnel barrier.

In Figure 4, we calculated the values of the resistance of MBT and BDT molecular devices. The mean resistance of MBT device was found to be 1.61 ± 0.45 kΩ and that of BDT junction was found to be 4.40 ± 1.78 kΩ, which show similar values within the error range. Also, we estimated the resistance per molecule using the molecular grafting density of BDT around 6.3×10^{14}/cm^2.[21, 22] And, we assumed grafting density of MBT is the same as BDT due to their identical backbone structure and similar molecular size. The estimated resistances per molecule were 143 ± 44 GΩ for BDT and 404 ± 176 GΩ for MBT devices. In general, the longer molecular length junctions have the higher resistance because the distance of tunnel barrier increases as molecular length increases. In this study, however, BDT molecular junction's resistance per molecule showed similar value to that of MBT junctions rather somewhat lower resistance than MBT junctions in spite of slightly longer molecular length than MBT (we estimated the molecular length using Chemdraw, MBT is 6.56 Å and BDT is 6.81 Å long). One of the reasons of this result might come from the fluctuation effect of the SAMs on the bottom electrode. Generally, the irregular fluctuation effect can suppress the subtle changes of electrical characteristics derived from molecular end-group. And another
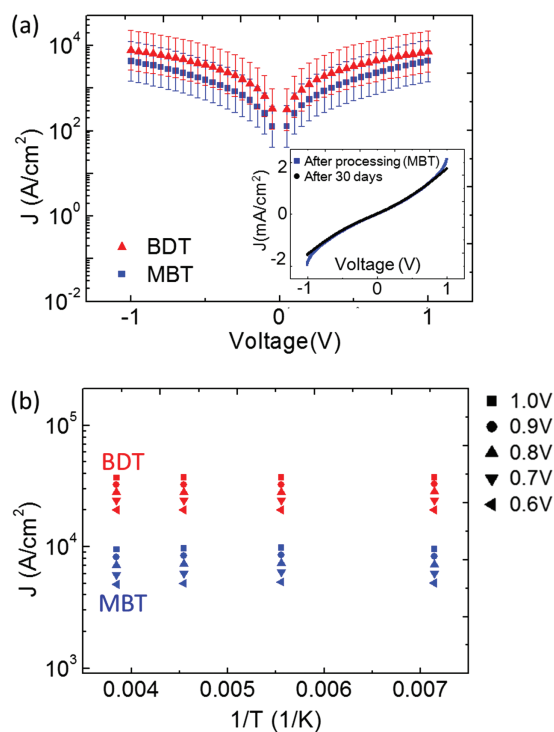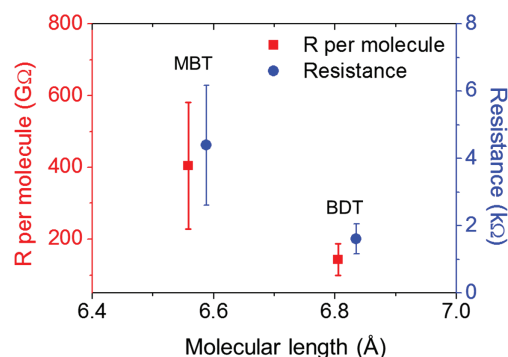

Figure 3. (a) Statistical J–V data of working BDT and MBT devices. (b) Arrhenius plot for BDT and MBT devices for various temperatures and voltages.

Figure 4. The determined resistance of MBT and BDT molecular devices (blue) and resistance per molecule (red).

reason can ben physical contact properties without any chemical bonding between graphene and molecular end group (–SH for BDT and –CH$_3$ for MBT). Generally, it is known that in the case of pure metal-molecule-metal junctions or metal-molecule-conducting polymer/metal junctions, the conductance difference is noticeable because changing molecular end-group results in difference in bonding nature between molecular end-group and top electrode at the interface.[13, 20, 23] However in our case, the bonding nature between graphene and SAM layer was the same as physisorbed contact. Whitesides' group have reported that the charge transport rate is 'insensitive' to end-group substitutions in molecule//Ga$_2$O$_3$/EGaIn junctions, suggesting that when only weak van der Waals force interacts at the interface, then it does not change the tunneling shape of the tunneling barrier.[24–26] Also, in the case of our study, –CH$_3$ and –SH end-group interacts with MLG film at the interface by weak van der Waals force without any chemical bonding. This weak physisorbed contact is not strong enough to affect to the charge transport characteristics. Therefore the electrical characteristics of our devices showed no significant differences.

4. CONCLUSION

In this study, we fabricated benzene-based MBT and BDT molecular devices with MLG electrode and compared the electrical characteristics of these two types of molecular devices. Although MBT and BDT have the same backbone structure and different end-group, their physisorbed contact properties at the interface between MLG electrodes produced no significant difference of electrical characteristics between two different types of junctions. The molecular electronics usually has focused on visible change of electrical characteristics by tuning molecules' end-group. However, our study supports insensitive charge transport nature in spite of end-group substitution in molecular electronic system where weak van der Waals force exerts on the physisorbed interface system. This investigation can help our understanding of electrical properties of molecular junctions with graphene electrodes towards reliable molecular electronic devices.

References and Notes

1. M. A. Reed and T. Lee (eds.), Molecular Nanoelectronics, American Scientific, Stevenson Ranch (**2003**).
2. A. Aviram and M. A. Ratner, *Chem. Phys. Lett.* 29, 277 (**1974**).
3. A. Nizan and M. A. Ratner, *Science* 300, 1384 (**2003**).
4. J. Chen, M. A. Reed, A. M. Rawlett, and J. M. Tour, *Science* 286, 1550 (**1999**).
5. J. E. Green, J. W. Choi, A. boukai, Y. Bunimovich, E. Johnston Halperin, E. Delonno, Y. Luo, B. A. Sheriff, K. Xu, Y. S. Shin, H.-R. Tseng, J. F. Stoddart, and J. R. Heath, *Nature* 445, 414 (**2007**).
6. C. P. Collier, E. W. Wong, M. Belohradský, F. M. Raymo, J. F. Stoddart, P. J. Kuekes, R. S. Williams, and J. R. Heath, *Science* 285, 391 (**1999**).
7. M. A. Reed, C. Zhou, C. J. Muller, T. P. Burgin, and J. M. Tour, *Science* 278, 252 (**1997**).
8. W. J. Liang, M. P. Shores, M. Bockrath, J. R. Long, and H. Park, *Nature* 417, 725 (**2002**).
9. A. Salomon, T. Böcking, J. J. Gooding, and D. Cahen, *Nano Lett.* 6, 2873 (**2006**).
10. X. Chen, S. Yeganeh, L. Qin, S. Li, C. Xue, A. B. Braunschweig, G. C. Schatz, M. A. Ratner, and C. A. Mirkin, *Nano Lett.* 9, 3974 (**2009**).
11. J. O. Lee, G. Lientschnig, F. Wiertz, M. Struijk, R. A. J. J. Janssen, R. Egberink, D. N. Reinhoudt, P. Hadley, and C. Dekker, *Nano Lett.* 3, 113 (**2003**).
12. T. Lee, W. Wang, J. F. Klemic, J. J. Zhang, J. Su, and M. A. Reed, *J. Phys. Chem. B* 108, 8742 (**2004**).
13. T. W. Kim, G. Wang, H. Lee, and T. Lee, *Nanotechnology* 18, 315204 (**2007**).
14. H. B. Akkerman, P. W. M. Blom, D. M. de Leeuw, and B. de Boer, *Nature* 441, 69 (**2006**).
15. G. Wang, Y. Kim, M. Choe, T. W. Kim, and T. Lee, *Adv. Mater.* 23, 755 (**2011**).
16. M. Min, S. Seo, S. M. Lee, and H. Lee, *Adv. Mater.* 25, 7045 (**2013**).
17. S. Seo, M. Min, S. M. Lee, and H. Lee, *Nat. Commun.* 4, 1920 (**2013**).
18. H. Jeong, D. Kim, P. Kim, M. R. Cho, W. Hwang, Y. Jang, K. Cho, M. Min, D. Xiang, Y. D. Park, H. Jeong, and T. Lee, *Nanotechnology* 26, 025601 (**2015**).
19. H. Jeong, W. Hwang, P. Kim, D. Kim, Y. Jang, M. Min, D. Xiang, H. Song, Y. D. Park, H. Jeong, and T. Lee, *Appl. Phys. Lett.* 106, 063110 (**2015**).
20. H. Yoo, J. Choi, G. Wang, T. W. Kim, J. Noh, and T. Lee, *J. Nanosci. Nanotechnol.* 9, 7012 (**2009**).
21. C. M. Whelan, M. R. Smyth, and C. J. Barnes, *Langmuir* 15, 116 (**1999**).
22. A. Salomon, D. Cahen, S. Lindsay, J. Tomfohr, V. B. Engelkes, and C. D. Frisbie, *Adv. Mater.* 15, 22 (**2003**).
23. H. Lee, H. Jeong, W.-T. Hwang, Y. Tchoe, G.-C. Yi, and T. Lee, *J. Nanosci. Nanotechnol.* 15, 5937 (**2015**).
24. H. J. Yoon, C. M. Bowers, M. Baghbanzadeh, and G. M. Whitesides, *J. Am. Chem. Soc.* 136, 16 (**2014**).
25. H. J. Yoon, N. D. Shapiro, K. M. Park, M. M. Thuo, S. Soh, and G. M. Whitesides, *Angewandte* 51, 4658 (**2012**).
26. C. M. Bowers, K.-C. Liao, H. J. Yoon, D. Rappoport, M. Baghbanzadeh, F. C. Simeone, and G. M. Whitesides, *Nano Lett.* 14, 3521 (**2014**).